Theoret. Appl. Mech., Vol.37, No.4, pp. 289–332, Belgrade 2010

Plasticity of crystals and interfaces: from discrete dislocations to size-dependent continuum theory

Sinisa Dj. Mesarovic *

Abstract

In this communication, we summarize the current advances in size-dependent continuum plasticity of crystals, specifically, the rate-independent (quasistatic) formulation, on the basis of dislocation mechanics. A particular emphasis is placed on relaxation of slip at interfaces. This unsolved problem is the current frontier of research in plasticity of crystalline materials. We outline a framework for further investigation, based on the developed theory for the bulk crystal.

The bulk theory is based on the concept of geometrically necessary dislocations, specifically, on configurations where dislocations pile-up against interfaces. The average spacing of slip planes provides a characteristic length for the theory. The physical interpretation of the free energy includes the error in elastic interaction energies resulting from coarse representation of dislocation density fields.

Continuum kinematics is determined by the fact that dislocation pile-ups have singular distribution, which allows us to represent the dense dislocation field at the boundary as a superdislocation, i.e., the jump in the slip filed. Associated with this jump is

*School of Mechanical and Materials Engineering, Washington State University, Pullman, WA 99164-2920, USA, e-mail: mesarovic@mme.wsu.edu

a slip-dependent interface energy, which in turn, makes this formulation suitable for analysis of interface relaxation mechanisms.

Keywords: grain boundary dislocations, discrete to continuum, long-range interactions, short dislocation-dislocation correlation.

1 Introduction

Investigation of mechanism of plastic deformation of metals, alloys and composites has a long history. Two recent reviews (McDowell 2008, 2010) offer a very broad perspective on models which traverse multiple length and time scales: atomic, dislocations, grain boundaries and multiple phases; as well as rate and temperature dependence. The focus of this paper is much narrower: the relationship between mechanics of discrete dislocations and time-independent (quasi-static) continuum theory for a single crystal and its interfaces. The time-independence is the consequence of time scale separation between two models. Dislocation move very fast, until arrested at an obstacle. From the point of view of experimental time scale of interest, the motion is practically instantaneous. Thus, it is dislocation statics, rather than dynamics, that is of primary interest. However, the separation of length scales, which has been the bedrock of classical size-invariant continuum theories, fails when the volume where dislocations move is restricted, resulting in size effects. Moreover, the reactions of dislocations and interfaces have significant effect on the energy of the system and plasticity with crystals. Two problems are reviewed in this paper:

(1) How to formulate a size-dependent continuum theory starting from mechanics of discrete dislocations?

(2) How to describe grain boundaries and interfaces, and their reactions with dislocations within continuum framework?

The problem (2) is largely unsolved. The available information is mostly qualitative; no general formulation encompassing various reactions exists. It is fair to state that the problem (2) represents the current frontier of knowledge in plasticity of crystalline materials. However, significant advances in addressing problem (1) have been accomplished

in the last two decades, and these provide a general framework to begin the analysis of problem (2).

1.1 Bulk plasticity of crystals

Earliest indications of discrete nature of plastic deformation were reported by Ewing & Rosenhain (1900), who observed the polycrystalline structure of metals, and slip steps on the surfaces of crystals. Their conclusion that the plastic deformation is pure shearing without volume change was later confirmed in numerous instances (e.g., Bridgman 1923, 1949). The first estimate of the shear strength of an ideal crystal (Frenkel, 1926) brought to light orders-of- magnitude discrepancy between this number and the experimentally observed yield stress. The puzzle of plastic deformation mechanisms was resolved by Orowan (1934), Polanyi (1934) and Taylor (1934), who independently discovered that it is the motion of dislocations that produces plastic deformation of crystals, rather than coherent sliding of atomic planes as assumed in Frenkel's calculations.

Study of dislocations as line defects in solids has grown into a theory of its own. In this limited space, we only note major milestones. A review of history as well as an extensive compendium of knowledge about dislocations is given in the Hirth & Lothe (1992) monograph. The solutions to elasticity problems, providing stress fields of dislocations with various geometries, were moved forward by Kröner's (1858) continuum theory of dislocations. The generalized forces driving the motion of dislocation lines have been studied by Peach & Koehler (1950), while the mechanism of multiplication of dislocations has been discovered by Frank & Read (1950). The wealth of knowledge was eventually combined into a computational model - discrete dislocation dynamics (Zbib et al, 1996, Hirth et al, 1996).

Once the mechanism of plastic deformation was discovered, the continuum theory of crystal plasticity was developed independently of dislocation theory. The key variables are continuum slip fields, one associated with each slip system. The slip systems are determined by the geometry of crystal lattice. The early model (Taylor, 1938) has been generalized

and given a rigorous mathematical form[1]. The first problem that required re-connection with dislocation theory is statistical hardening by dislocation interactions. The theoretical developments (Ortiz & Popov, 1982) and extensive experimental results[2] have yielded comprehensive models[3]. The resulting theory is a simple continuum, without intrinsic length scale.

That size of crystals determines its yield strength has been known since 1950's (Hall, 1951, Petch, 1953). Ashby's (1970) analysis of size effects in precipitation hardened metals, and development of the concept of geometrically necessary dislocations provided new impetus to experimental studies. The size effects were observed in numerous experiments[4]. To model the size effects, a number of phenomenological mathematical formulations have been proposed during the last two decades. The theories include higher order kinematic gradients, which, in turn, require characteristic length(s) (Mindlin, 1964, Aifantis, 1987), and inevitably produce qualitative prediction of size effect. The higher order gradients are typically related to Nye's (1953) dislocation density tensor. While this choice is intuitive, it is by no means unique. Moreover, the characteristic lengths are typically phenomenological, without clear physical meaning that can be connected to dislocation mechanics. After the pioneering models Fleck & Hutchinson[5], the major contribution was made by Gurtin (2000, 2002, 2003), who observed that the correct thermodynamic formulation requires that work conjugate of slip be independent from the stresses. More recently, the focus has been shifted to interfaces[6], with particular emphasis on dissipative models. However, analyses are mostly on the continuum level; starting from phenomenological assumptions, mathematical consequences are explored.

---

[1]Hill (1966), Hill & Rice (1972), Asaro & Rice (1977), Hill & Havner (1982)

[2]Franciosi et al (1980), Franciosi & Zaoui (1982), Franciosi (1983, 1985)

[3]Bassani & Wu (1989), Cuitino & Ortiz (1993), Bassani (1994).

[4]Gane & Cox (1970), Pethica et al (1983), De Guzman et al (1993), Stelmashenko et al (1993), Fleck et al (1994), Ma & Clarke (1995), Poole et al (1996), Stolken & Evans (1998).

[5]Fleck & Hutchinson (1993, 1997), Smyshlyaev & Fleck (1996).

[6]Gudmundson (2004), Aifantis & Willis (2005), Frederiksson & Gudmundson (2007), Fleck & Willis (2009).

Attempts to fit the predictions of a theory to either experiments[7] or simulations[8] indicate a need for more rigorous approach, i.e., a derivation of a continuum theory by systematically coarsening dislocation mechanics. Advances in statistical analysis of collective dislocation behavior[9] have resulted in statistical continuum dislocation dynamics formulations[10]. Such formulations emphasize dynamics of dislocation motion, while representing dislocations as continuum density fields. The key ingredient stems from the attempt to resolve the fundamental problem of discrete dislocation dynamics: long-range interactions. This is achieved by computing a local approximation to the driving force (the Peach-Koehler force). The basis for this approximation is the assumption that dislocation-dislocation correlation function is short-range (Groma, 1997).

1.2 Plasticity at crystal interfaces

The importance of grain boundaries has been long recognized and much effort has been expanded to understand their structure and energies. The accomplishments until mid-nineties have been compiled in the monograph by Sutton & Balluffi (1995). Extensive studies of interface energies, texture evolution during grain growth and processing, solute-interface interactions, grain boundary mobility, stress concentrations, and other problems, have been done by the MIMP group. An extensive list of references can be found on the group's website[11].

They have identified a number of boundaries that would be considered low-energy or high-energy structures. In general, the symmetric boundaries with high density lattice planes along the boundary have lower energy[12].

Macroscopically, the geometric structure of an interface is described

[7] Fleck et al (1994), Nix & Gao (1998), Stolken & Evans (1998), Sun et al (2000).

[8] Bassani et al (2001), Shu et al (2001), Bittencourt at al (2003), Ohashi (2004).

[9] Groma (1997), Zaiser at al (2001), Groma et al (2003).

[10] Arsenlis et al (2004), Yefimov et al (2004), Groma et al (2006, 2007), Limkumnerd & Van der Giessen (2008).

[11] http://mimp.mems.cmu.edu/publications/index.html

[12] Dillon et al (2010), Rohrer & Miller (2010), Adams et al (1999).

by five parameters: three for relative orientation of two crystals and two for interface orientation. Microscopically, a relaxation takes place within the interface and up to 4 additional parameters are needed[13]. Several description of interface structure are available, the most commonly used being the coincidence site lattice (CSL) (Bollman, 1970) and structural units (Sutton & Vitek, 1983). The most important for calculating the elastic energy of the system is the representation based on a suitable intrinsic defect structure which may include intrinsic dislocations, disconnections, and disclinations[14].

While these *intrinsic* defects have received much attention as a description of the interface geometry, comparatively little has been done to understand the reaction of an *extrinsic* dislocation with a given interface defect structure. Notable exception is the work done by Priester and coworkers[15]. Few computational atomistic studies have done for the problem of dislocation approaching an interface (Pestman et al, 1991, Chen et al, 1993). More recent work has been focused on nucleation of dislocations from grain boundaries[16]. The computations are typically limited to simple geometries, such as tilt boundaries with high symmetry. In summary, what is known is that dislocation impinging on a boundary can interact with it in several ways, including absorption of dislocation, core spreading, dissociation into sessile and mobile dislocations, and transmission through the boundary with associated residual defects. What is not known is: (i) if the set of possible reactions is complete, and, (ii) except in few special cases of tilt boundaries, under which conditions (stress, temperature) each of the mechanism operates.

Some possible dislocation-interface reactions are illustrated in Figure 1. Note that the reactions often involve non-conservative motion, and that the paths in configurational space are unknown. Extensive atomistic level studies are needed to map the space of possible dislocation-grain boundary reactions.

---

[13]Fortes (1972), Adams & Field (1992), Field & Adams (1992)

[14]Pond & Vlachavas (1983), Clarke et al (1992), Priester (2001), Pond at al (2003, 2007), Hirth et al (2006, 2007), Akarapu et al (2008).

[15]Poulat et al (1998, 2001), Priester (2001), Couzinie et al (2003, 2004, 2005),

[16]Spearot et al (2005, 2007 a, b), Tschopp et al (2008).

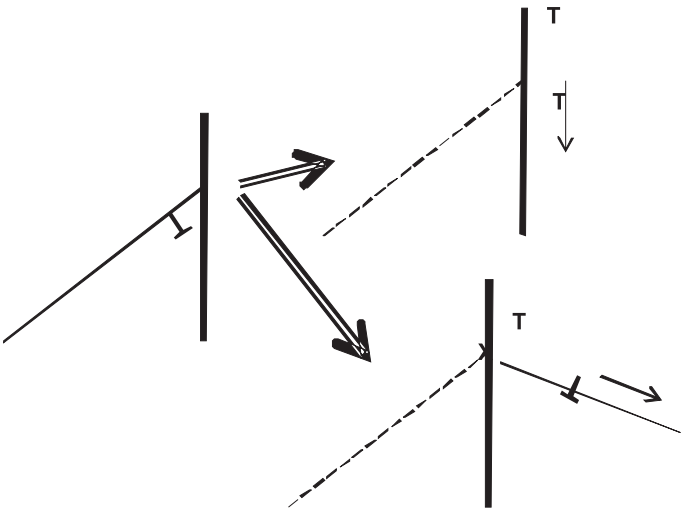

(a) Single dislocation impinging on a tilt boundary could be accommodated within the interface and dissociate into sessile and mobile components (up), or, it can transmit (down), i.e. nucleate dislocation in the other crystal leaving an interface dislocation and disconnection (X).

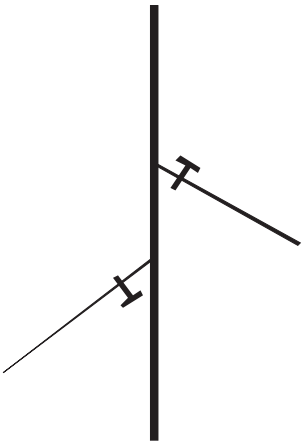

(b) Two dislocations impinging on a tilt boundary from different sides.

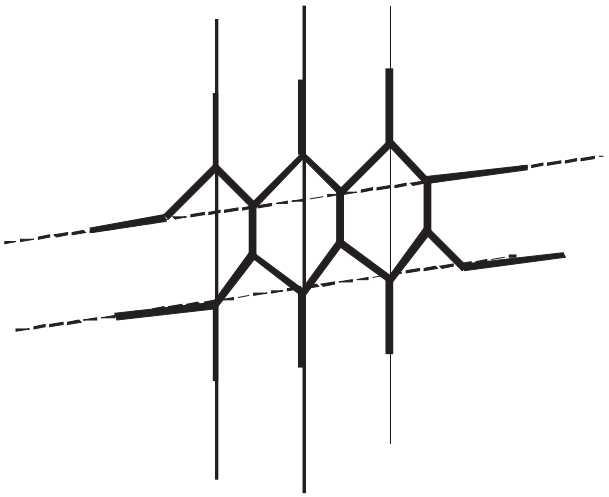

(c) A reaction that may occur on a twist boundary, or on a tilt boundary if different slip systems are active on two sides of the interface. Two sets of dislocations impinge from different sides (thin solid and dashed lines). The reaction product is shown as network of thick lines. It has been observed in Ni $\Sigma 11\{311\}$ boundary (Poulat et al, 2001, Priester, 2001).

Figure 1: Sketches of dislocation-interface reactions of increasing complexity.

The paper is organized as follows. In Section 2, a short summary of dislocation theory is given, followed by summary of different kinematic descriptions of dislocations in Section 3, and an overview of Kroner's continuum theory of dislocations in Section 4. Standard size-invariant continuum crystal plasticity is summarized in Section 5, with emphasis on results relevant for thermodynamic coarsening, which is described in Section 6. In Section 7, the outline of the size-dependent continuum formulation, without bulk or interface relaxations, is given. Finally, in Section 8, relaxation and dissipation resulting from dislocation-dislocation and dislocation-interface reactions is discussed.

The analysis is limited to isotropic elasticity, linearized kinematics ("small strain" theory), and isothermal processes.

2 Selected elements of dislocation mechanics

Dislocation is line across which a lattice discontinuity with respect to the perfect crystal takes place. The discontinuity is quantified by the Burgers vector. The standard local definition of the Burgers vector, $\mathbf{b}$, is not unique. It depends on the local direction of the dislocation line, characterized by the unit tangent vector, ξ (Hirth & Lothe, 1992). The pairs $(\mathbf{b}, \xi)$ and $(-\mathbf{b}, -\xi)$ describe the same discontinuity. Our current purpose requires a more precise definition, such that can be uniquely related to the continuum plasticity slip field. This definition is illustrated in Figure 2.

A planar cut π through the solid is oriented by the unit normal $\mathbf{m}$, which points to the *upper* half space. The dislocation loop C is oriented by unit tangent vector ξ so that it circles in the counterclockwise sense when seen from the upper side. Within the region bounded by C, the upper half space slips uniformly by $\mathbf{b}$, commensurate with the lattice periodicity in this particular direction, so that the crystal lattice inside the loops remains unchanged and the discontinuity occurs only along the dislocation line.

Dislocation segment ξds, with the Burgers vector orthogonal to ξ is

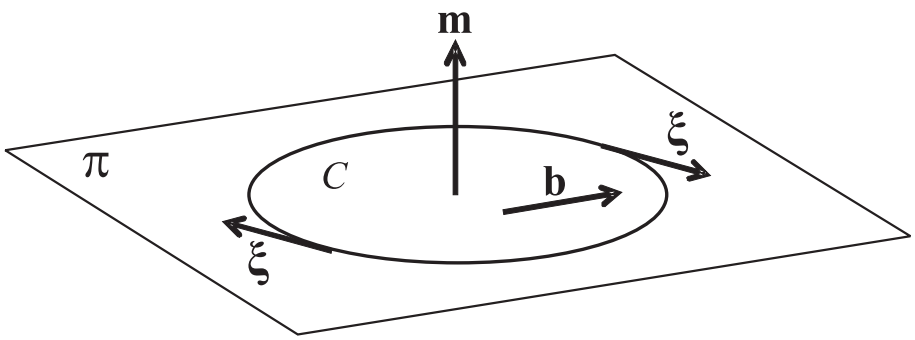

Figure 2: Definition of dislocation line direction and Burgers vector.

an *edge* segment, while the one with Burgers vector parallel to ξ is a *screw* segment. General segments can be thought of as having an edge and a screw component.

Once the initial choice of direction $\mathbf{m}$ is made (which has to be done in continuum theory anyway), the line direction and the Burgers vector are defined uniquely. Moreover, as will be seen later, it provides a framework for handling super-dislocations (i.e., multiple collinear dislocations) and dislocation walls at the interfaces.

We consider the interaction energy of two dislocation loops, C_σ and C_τ in an infinite isotropic elastic space with shear modulus μ and the Poisson ratio ν. The position vectors of loop points are $\mathbf{x} \in C_\sigma$ and $\mathbf{x}' \in C_\tau$. The corresponding Burgers vectors are $\mathbf{b}$ and $\mathbf{b}'$, respectively. Let R be the magnitude of the relative position vector $\mathbf{R} = \mathbf{x}' - \mathbf{x}$. We define the unit direction vector $\mathbf{d} = \mathbf{R}/R$ and the rank-two tensor $\mathbf{T}$:

$$T_{ij} = \delta_{ij} - d_i d_j. \tag{1}$$

Index notation with summation over repeated lower indices is used, unless otherwise noted. The elastic interaction energy between the two loops is given by (Hirth & Lothe, 1992):

$$\begin{aligned} E^{\sigma\tau} &= \frac{\mu}{2\pi} \oint\limits_{C_\sigma} \oint\limits_{C_\tau} \frac{ds ds'}{R} \left[(\mathbf{b}' \cdot \xi)\,(\mathbf{b} \cdot \xi') - (\mathbf{b} \cdot \xi)\,(\mathbf{b}' \cdot \xi') \right. \\ &\quad \left. + \frac{1}{2(1-\nu)}\,(\mathbf{b} \times \xi) \cdot \mathbf{T} \cdot (\mathbf{b}' \times \xi') \right]. \end{aligned} \tag{2}$$

The integrand represents the interaction energy between two segments ds and ds'. The self energy of a single loop is obtained as the sum of elementary interaction energies between segments, i.e., the two integrations in (2) are performed over the same line and the result is multiplied by $1/2$ to account for double counting of segment pairs.

It is evident from (2) that the interaction energy between segments is dependent on the edge/screw character of segments. Therefore, this distinction must be preserved in the continuum kinematics.

The long-range nature of interactions is clearly seen in (2). Segments interaction energy is proportional to $1/R$, which makes the total energy of the system irreducibly non-local, i.e., there is no cutoff distance beyond which interactions can be neglected. Moreover, this non-locality in an infinite space, implies the dislocation-boundary interactions in any finite domain.

This has significant implications for calculating the total free energy of solid with dislocations. It is also a major obstacle to application of dislocation dynamics simulations to all but small domains and simple boundary conditions (e.g., periodic).

Stresses caused by the existence of a segment of dislocation loop C, scale with $1/R^2$. With the same notation as above (Hirth & Lothe, 1992):

$$\sigma(\mathbf{x}', C) = \frac{\mu}{4\pi} \oint_C \frac{ds}{R^2} \left[(\mathbf{d} \times \mathbf{b})\xi + \xi(\mathbf{d} \times \mathbf{b}) - \frac{1}{2(1-\nu)} (\mathbf{Q} \times \mathbf{b}) \cdot \xi \right], \tag{3}$$

where the component of the rank-three tensor $\mathbf{Q}$ are: $Q_{pqi} = \delta_{pq} d_i - \delta_{pi} d_q - \delta_{qi} d_p + d_p d_q d_i$.

Dislocations typically move within their slip plane. This motion is called *glide* and produces a volume conserving plastic deformation. At high temperature, dislocations can *climb* out of their slip planes. This requires diffusion of vacancies and is not volume conserving. If the intersection of two slip planes is parallel to the Burgers vector in one plane, screw segments can *cross-slip*, i.e., switch their glide plane. Typically, the driving force for gliding in the original plane is larger so that the second cross slip takes place. The new short segment is created in the

plane parallel to the original plane and acts as the source which emits further loops in the new plane. Such *double cross-slip* is the primary mechanisms for multiplication of dislocations in a deforming body.

The driving force for dislocation motion depends on the stresses, both externally applied and caused by other dislocation (3). The force $d\mathbf{f}$ acting on the segment $\xi ds$with Burgers vector $\mathbf{b}$ is

$$d\mathbf{f} = (\mathbf{b} \cdot \sigma) \times \xi ds. \tag{4}$$

While moving through a crystal, dislocation segments:

(i) Interact elastically, i.e., the stress field of one repulses or attracts the other, according to (4), and,

(ii) If close enough, react to form a new dislocation segment, with a lower elastic energy. Two parallel segments: $(\xi\Delta s, \mathbf{b}^I)$ and $(\xi\Delta s, \mathbf{b}^{II})$, form the new segment: $(\xi\Delta s, \mathbf{b}^R = \mathbf{b}^I + \mathbf{b}^{II})$, if such reaction is energetically favorable. Note that the segments must be oriented in the same direction. Otherwise the signs in the sum should be changed. Similar reaction can occur between dislocations across the interface, and between a dislocation and an intrinsic grain boundary dislocation.

3 Kinematic coarsening

The densities of geometrically necessary (GN) dislocations can be represented by Nye's (1953) dislocation density tensor field $\mathbf{A}(\mathbf{x})$. In an infinitesimal volume element dV, about the point $\mathbf{x}$, we consider segments of dislocations of type s, with the Burgers vector $\mathbf{b}^s$, and the unit tangent vector ξ^s. Let $\rho^s(\mathbf{x})dV$ be the total length of dislocation segments of type s in dV. Then:

$$\mathbf{A} = \sum\nolimits_s \rho^s \mathbf{b}^s \xi^s. \tag{5}$$

The expression $\mathbf{b}^s\zeta^s$ denotes a dyadic product, so that the components of $\mathbf{A}(\mathbf{x})$ are given by $A_{ij} = \sum_s \rho^s b_i^s \xi_j^s$.

To illustrate different representations of GN dislocations, we consider a simple two-dimensional problem: an infinite thin film sandwiched between elastic half-spaces, as shown in Figure 3. The only non-vanishing component of Nye's tensor for the case of edge dislocations piling-up in slip planes orthogonal to the boundary is A_{13}.

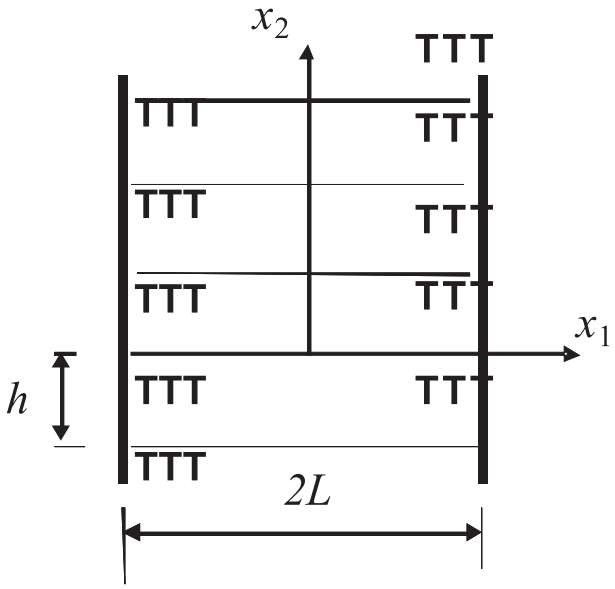

Figure 3: An elastic-plastic thin film with single slip system and slip planes orthogonal to the boundary is sandwiched between elastic half spaces. The interfaces are impenetrable to dislocations. Slip planes are equidistant (h) and the film is infinite in x_2 direction. All dislocations are edge with the magnitude of Burgers vector b.

We differentiate between three types of kinematic representations of the GN dislocations:

(i) *Discrete representation* is mathematically represented as

$$\hat{A}_{13}(x_1, x_2) = -b \sum_j \sum_{k=-\infty}^{\infty} sign(x_1^j) \delta(x_1^j) \delta(x_2 - kh), \qquad (6)$$

where x_1^j are x_1- coordinates of individual dislocations, δgs the Dirac delta function, and h is the distance between slip planes (Figure 3).

(ii) *Semi-discrete representation* is obtained by smearing out the Burgers discontinuity in the slip plane, but keeping the slip planes discrete:

$$\bar{A}_{13}(x_1, x_2) = B(x_1) \sum_{k=-\infty}^{\infty} \delta(x_2 - kh). \tag{7}$$

(iii) *Continuous representation* is obtained from the semi-discrete one by smearing out B in the direction normal to the slip planes. For the simple problem shown in Figure 3, this representation is easily related to the semi-discrete one:

$$A_{13}(x_1) = B(x_1)/h. \tag{8}$$

4 Continuum kinematics and incompatibility

Motion of dislocations in their slip planes, results in plastic deformation. Slip system is characterized by the slip plane and slip direction. The plastic deformation associated with a slip system is described by a scalar fieldg− slip.

To emphasize the distinction between the screw and edge components of dislocation segments, we use the notation different from the standard crystal plasticity notation[17]. The slip system α is defined by the unit normal $\mathbf{m}^\alpha$, and two orthogonal in-plane unit vectors. The slip direction $\zeta_\circ^\alpha$ is parallel to the Burgers vector of dislocations that move in the slip system. It is the direction of a screw segment. The direction of an edge segment $\zeta_\perp^\alpha$ is orthogonal to the Burgers vector, so that (Figure 4):

$$\zeta_\perp^\alpha \times \zeta_\circ^\alpha = \mathbf{m}^\alpha. \tag{9}$$

[17]The triad $(\zeta_\circ^\alpha, \mathbf{m}^\alpha, \zeta_\perp^\alpha)$ is usually denoted as $(\mathbf{s}^\alpha, \mathbf{m}^\alpha, \mathbf{t}^\alpha)$.

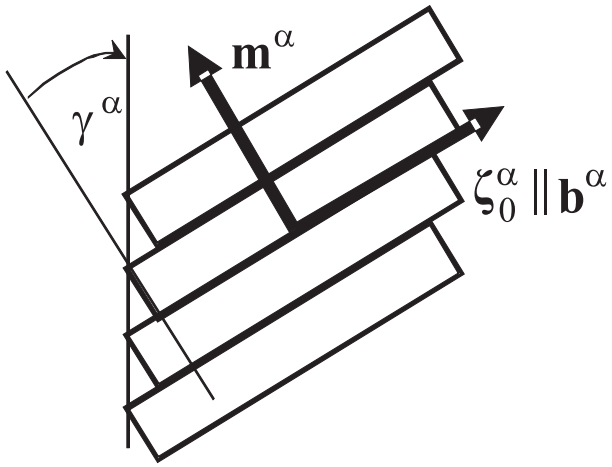

Figure 4: Base vectors for the slip system α.

The slip fields $\gamma^\alpha(\mathbf{x})$, on all active slip systems, combine to produce the slip tensor:

$$\gamma(\mathbf{x}) = \sum\nolimits_\alpha \gamma^\alpha \zeta_\circ^\alpha \mathbf{m}^\alpha, \tag{10}$$

whose symmetric portion, $S(\gamma) = \frac{1}{2}(\gamma + \gamma^T)$, is the plastic strain.

Both, the elastic strain $\mathbf{e}$, and the plastic strain $S(\gamma)$, are incompatible, i.e., taken separately, neither is a symmetric part of a gradient of a single-valued displacement field. Kroner's (1958) incompatibility tensor, η, is the measure of incompatibility of elastic strain:

$$\begin{aligned} &\mathrm{Inc}(\mathbf{e}) \equiv \nabla \times \mathbf{e} \times \nabla = \eta \neq 0, \\ &\eta_{ij} = \in_{ipm} \in_{jnq} e_{mn,pq}, \end{aligned} \tag{11}$$

where $\in_{ipm}$ is the alternating symbol. The indices after a comma represents partial derivatives: $\partial a_i / \partial x_j = a_{i,j}$. The sum of the elastic and plastic strains must be compatible:

$$\mathrm{Inc}(\mathbf{e} + S(\gamma)) = 0 \tag{12}$$

The Nye's (1953) dislocation density tensor, $\mathbf{A}$, quantifies the accumulation of dislocations, i.e. the non-vanishing net Burgers vector in the

volume element. Kroner (1981) showed that

$$\mathbf{A} = -\gamma \times \nabla. \tag{13}$$

The relation between the gradients of slip on the slip systemgα and the Nye's tensor can be specified more precisely, in a way that relates components of the gradient to the densities of edge and screw GN dislocations. Define the in-plane unit tensor for the slip system α:

$$\mathbf{P}^{\alpha} = \mathbf{I} - \mathbf{m}^{\alpha}\mathbf{m}^{\alpha} = \zeta_{\circ}^{\alpha}\zeta_{\circ}^{\alpha} + \zeta_{\perp}^{\alpha}\zeta_{\perp}^{\alpha}. \tag{14}$$

It acts as a projection operator, such that the projection of an arbitrary vector $\mathbf{a}$ on the slip plane α is $\mathbf{P}^{\alpha} \cdot \mathbf{a}$. The in-plane gradient operator is then defined as

$$\overset{\alpha}{\nabla} = \mathbf{P}^{\alpha} \cdot \nabla. \tag{15}$$

The in-plane slip gradient vector is

$$\mathbf{g}^{\alpha} = \overset{\alpha}{\nabla}\gamma^{\alpha} = \nabla \cdot (\mathbf{P}^{\alpha}\gamma^{\alpha}) = g_{\perp}^{\alpha}\zeta_{\circ}^{\alpha} + g_{\circ}^{\alpha}\zeta_{\perp}^{\alpha}. \tag{16}$$

The component, $g_{\perp}^{\alpha}$, quantifies the density of edge dislocations, while the component$g_{\circ}^{\alpha}$, quantifies the density of screw dislocations. The Nye's tensor is then obtained as

$$\mathbf{A} = -\sum\nolimits_{\alpha} (g_{\perp}^{\alpha}\zeta_{\circ}^{\alpha}\zeta_{\perp}^{\alpha} - g_{\circ}^{\alpha}\mathbf{P}^{\alpha}). \tag{17}$$

In elastic-plastic crystals the incompatibility arises from the non-vanishing net Burgers vector, so that Kroner's incompatibility tensor η, must be related to the Nye's tensor. From (12, 13), and using the linearity of operators Inc and S, Kroner (1958) obtained:

$$\eta = S(\nabla \times \mathbf{A}). \tag{18}$$

It follows from (11, 13) that, if the Nye's dislocation density field $\mathbf{A}(\mathbf{x})$ is prescribed, then the stress σ must satisfy

$$\mathrm{Inc}(\mathbf{C}^{-1} : \sigma) = S(\nabla \times \mathbf{A}), \tag{19}$$

in addition to the standard equilibrium equations. In (19), $\mathbf{C}^{-1}$is the elastic compliance tensor, i.e., the inverse of the elastic stiffness tensor, $\mathbf{C}$.

For given dislocation density field $\mathbf{A}$, Kroner's incompatibility equations (19) , are solvable in terms of stress potentials, with traction boundary conditions. With other boundary conditions, the solution is more difficult to obtain. Moreover, the field $\mathbf{A}$ can be given as discontinuous and can represent an assembly of discrete dislocations. Indeed, many of the solutions to discrete dislocation problems (Hirth & Lothe, 1992) have been obtained using Kroner's formalism, following from (19), and applied to an infinite space.

5 Size-invariant crystal plasticity

In order to construct a size-dependent continuum theory, we begin with thermodynamic analysis of the standard size-invariant crystal plasticity formulation. More precisely, we analyze the free energy of a plastically deformed crystal, as might be computed from different descriptions of dislocations, listed in Section 3.

Consider the finite volume V, bounded by the surface S. The weak form (principle of virtual work) of the classical crystal plasticity can be written as:

$$\delta W = \int_V \left[\sigma : \delta\mathbf{e} + \sum\nolimits_\alpha \tau^\alpha \delta\gamma^\alpha\right] dV = \int_S \mathbf{t}\cdot\delta\mathbf{u} dS. \tag{20}$$

The first term with elastic strain $\mathbf{e}$, and the corresponding stress $\sigma = \mathbf{C} : \mathbf{e}$, is the variation of the elastic strain energy:

$$\Phi = \frac{1}{2}\int_V \mathbf{e} : \mathbf{C} : \mathbf{e}\ dV, \tag{21}$$

The second term in (20) includes dissipation, as well as the statistically stored energy, which is considered mechanically irreversible (Mesarovic, 2005). Standard analysis of the weak form implies that the work conjugate of slip, τ^α, is equal to the resolved shear stress τ^α_R:

$$\tau^\alpha = \tau^\alpha_R = \mathbf{m}^\alpha \cdot \sigma \cdot \zeta^\alpha_\circ. \tag{22}$$

The last expression is also interpreted as the yield condition for slip system α.

The total elastic strain $\mathbf{e}$ is incompatible in the sense of (11). In general, there is infinity of partitions into the compatible strain $\mathbf{E}$ and the incompatible strain ε:

$$\mathbf{e} = \mathbf{E} + \varepsilon : \ \mathrm{Inc}(\mathbf{E}) = 0 \text{ and } \mathrm{Inc}(\varepsilon) = \mathrm{Inc}(\mathbf{e}) = \eta. \tag{23}$$

However, the condition that $\mathbf{E}$and ε are *orthogonal* in V:

$$\int_V \mathbf{E} : \mathbf{C} : \varepsilon \ dV = 0 \tag{24}$$

(i.e., that the stress corresponding to one does no work on the other), renders a unique partition (23). The proof is given in Mesarovic et al (2010).

Orthogonality implies that the strain energies corresponding to the two fields are additive:

$$\Phi = \Phi_c + \Phi_{inc} = \frac{1}{2}\int_V \mathbf{E} : \mathbf{C} : \mathbf{E} \ dV + \frac{1}{2}\int_V \varepsilon : \mathbf{C} : \varepsilon \ dV. \tag{25}$$

In crystal plasticity, incompatibility is the result of non-vanishing Nye's tensor (4), so that the incompatible strain energy Φ_{inc} is, in fact, identical to *the microstructural energy* (Mesarovic, 2005), defined as the elastic interaction energy between the GN segments. Specifically, when dislocated (elastic-plastic) solid is embedded in an infinite elastic matrix, and with elastic moduli of the matrix identical to those of the dislocated solid, the microstructural energy can be expressed as double convolution of a quadratic form of either Kroner's incompatibility tensor (Kosevich, 1979), or of Nye's tensor (Rickman & LeSar, 2001, Mesarovic, 2005):

$$\Phi_{inc} \equiv W^m = \frac{1}{2}\int_V dx^3 \int_V d\xi^3 \mathbf{A}(\mathbf{x}) : \mathbf{M}(\mathbf{x} - \xi) : \mathbf{A}(\xi), \tag{26}$$

where the two-point rank-four tensor field $\mathbf{M}$ is given as

$$M_{ijkl} = \frac{2\mu}{8\pi R}(2\delta_{jk}\delta_{il} - \delta_{ij}\delta_{kl}) + \frac{\bar{E}}{8\pi R} \in_{pij} \in_{qkl} (\delta_{pq} - d_p d_q). \tag{27}$$

In (27), $\bar{E}$ is the plane strain modulus: $\bar{E} = 2\mu/(1-\nu)$. The formulation (26) is convenient for computing energies of stacked dislocation pile-ups (Yassar et al, 2007, Baskaran et al, 2010).

It bears emphasis that the elastic interaction energy of dislocations (26), as computed using continuum field $\mathbf{A}(\mathbf{x})$, is already included in the solution to the standard, size-invariant crystal plasticity (20, 25).

For other boundary conditions, the long-range nature of dislocation interactions, implies that computation of the microstructural energy requires computation of generalized image dislocations (Khraishi & Zbib, 2002a,b) which enforce the particular boundary condition. In general, this amounts to solving singular integral equations, but simplifying approximations are possible. The formulations for various boundary conditions are given in Mesarovic (2005), as are the simplifying approximations. At present, it suffices consider an elastic-plastic crystal embedded into an infinite elastic medium with identical elastic properties. Later, we will be able to generalize the conclusions.

Nye's (1953) coarsening (5, 8), as well as the in-plane coarsening (7), are purely kinematic. There is no a priori reason why the energies computed from (7) or (8) should be good approximations to the energy computed from (6). Roy et al (2007) demonstrated that the error resulting from such approach is significant. It is this difference in energies – *the coarsening error in microstructural energy* that provides the physical justification for the appearance of characteristic lengths.

Since $\Phi_{inc} \equiv W^m$, the weak form of the crystal plasticity can be written as

$$\delta W = \delta\Phi_c + \int_V \sum\nolimits_\alpha \tau^\alpha \delta\gamma^\alpha dV + \delta W^m = \int_S \mathbf{t}\cdot\delta\mathbf{u}\; dS. \qquad (28)$$

The discrete representation (6) gives the most accurate values of energy. Therefore, we seek the error in microstructural energy that results from replacing the discrete dislocation distribution (6) with the continuous field (5, 8).

$$\Delta W^m = W^m(\hat{\mathbf{A}}) - W^m(\mathbf{A}). \qquad (29)$$

This is the portion of free energy that is missing from the classical crystal plasticity. The expression for the virtual work will then have the

form:

$$\delta W = \int_V \left[\sigma : \delta\mathbf{e} + \sum\nolimits_\alpha \tau^\alpha \delta\gamma^\alpha\right] dV + \delta\Delta W^m = \int_S \mathbf{t}\cdot\delta\mathbf{u}\; dS. \qquad (30)$$

The continuum fields σ, $\mathbf{e}$ and γ^α in (24) are computed using the continuous representation (5, 8).

Owing to the type of dependence $\mathbf{M}(\mathbf{x}-\xi)$, the double convolution (26) cannot be reduced to a local form, i.e., cannot be approximated by a local expression of the type $W^m = \int_V \omega(\mathbf{A}(\mathbf{x}))dV$, which would lead to a local constitutive law. This property is the direct result of long-range interactions, which are evident in the discrete form (2). Fortunately, the error in microstructural energy (29) is reducible to a local form.

6 Approximation for the coarsening error in microstructural energy

Consider the two-dimensional configuration shown in Figure 5: elastic-plastic thin-film embedded into an elastic space, with identical properties. The inclined slip planes contain pile-ups of dislocations at the boundary.

In isotropic elasticity, the problems of edge (plane strain) and screw (anti-plane) dislocations are orthogonal and stresses, strains and energies are additive (Hirth & Lothe, 1992). The general case with arbitrary Burgers vectors is obtained by superposition of the two basic problems. We consider pile-up configurations against the impenetrable boundaries.

The dislocation distribution in the pile-up has a crack tip type singularity. Thus, when boundary surfaces have small curvatures, the problems are essentially two-dimensional, much like crack tip problems.

Finally, we consider equally spaced slip planes. This is, of course, an approximation. We expect that it is the first order approximation, and that the corrections will depend on the higher order moments of the probability distribution of spacings. This approximation notwithstanding, the solutions obtained using the configuration in Figure 5 can be used to make general conclusions about interaction energies of pile-ups.

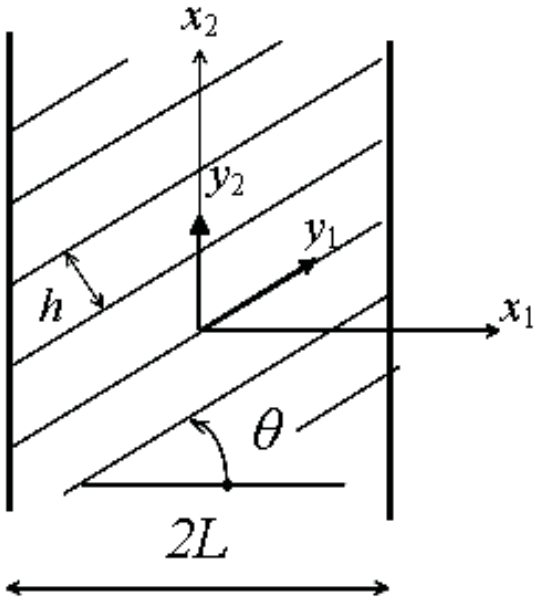

Figure 5: Constrained shear of a thin film with a single slip system.

Using this configuration, Baskaran et al (2010) have recently shown that, for a wide range of parameters, kinematic and thermodynamic differences between the discrete (6) and semi-discrete (7) representations are negligible. The major difference in energies arises from the coarsening in the direction normal to the slip plane, i.e., as the difference between energies computed from the continuous (5, 8) and the semi-discrete (7) representation, so that (29) can be approxiamted as

$$\Delta W^m \approx W^m(\bar{\mathbf{A}}) - W^m(\mathbf{A}). \tag{31}$$

Moreover, while the total microstructural energy is irreducibly non-local [cf. (2, 26)], its error can be localized (Mesarovic et al, 2010). This is readily understood if one considers a single dislocation represented either as discrete (Dirac delta), or smeared into dislocation density over a small region. At a distance much larger than the smearing region, the stresses and elastic energy densities will be identical in both cases, but will not vanish. Thus, while the influence of a dislocation is long-range,

the error arising from approximating the dislocation with a smeared distribution is short range, and consequently, subject to local approximation.

Away from the boundaries, where the dislocation densities vary slowly, the energy error has a simple continuum representation as a quadratic form of Nye's components (5), or slip gradients (16) (Mesarovic at al, 2010). This contribution to the coarsening energy error (31) has the form

$$\frac{1}{2}\int_V \mathbf{g}^\alpha \cdot \mathbf{D}^{\alpha\alpha} \cdot \mathbf{g}^\alpha dV.$$

Near the boundary, a different kinematic approximation is needed to represent singular dislocation distribution fields.

In defining a continuum theory, the economy of computations must be considered. After all, if continuum computations are not economical, then why not simply model the problem using discrete dislocation mechanics? Should we keep the singular gradients near the boundary, the required dense discretization in any numerical method would all but defeat the purpose of defining the continuum theory. Therefore, an approximation that avoids dense meshing required for resolving singular gradients is desired. Such approximation illustrated in Figure 6, where the sharp concentration of slip gradients at boundaries is approximated by a finite jump in slip at the boundary. The slowly-varying slip distribution in the interior remains.

The characteristic length that emerges from these calculations is the (average) spacing of slip planes, h in Figure 5. This length evolves during deformation; dislocations spread to new parallel slip planes by means of the double cross slip mechanism (Hirth & Lothe, 1992). Moreover, there will be a characteristic length associated with each active slip system. The initial value for an annealed crystal is large; it is of the order of density for Frank-Read sources, As dislocations spread onto new planes, the average spacing will be weighted average of two lengths: the initial spacing of sources and the characteristic cross-slip distance, the latter being the saturation value.

If the singular dislocation density $\mathbf{g}^\alpha$ (16) is to be replaced at the boundary by the appropriate boundary value of slip, the geometry at

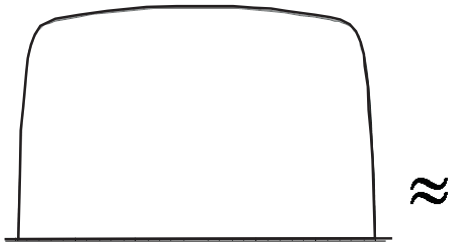

(a) Typical slip distribution between impenetrable boundaries using the semi-discrete problem formulation. At the boundaries, the slip gradient is singular.

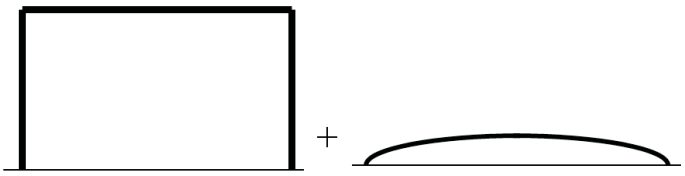

(b) Approximation to the actual slip distribution. Singular gradients at the boundaries are approximated by jumps (step functions), so that the approximate slip field consists of slowly varying portion with non-vanishing boundary values.

Figure 6

the intersection of slip plane and the boundary must be defined. Let $\mathbf{n}$ be the outer unit normal to the boundary. The slip plane is bounded by the intersection with the boundary C. The outer unit normal to the trace C can be written as

$$\mathbf{N}^\alpha = \frac{\mathbf{P}^\alpha \cdot \mathbf{n}}{|\mathbf{P}^\alpha \cdot \mathbf{n}|} = \cos\phi^\alpha \zeta_\circ^\alpha + \sin\phi^\alpha \zeta_\perp^\alpha, \;\; |\mathbf{P}^\alpha \cdot \mathbf{n}| = |\mathbf{n} \times \mathbf{m}^\alpha| = \cos\theta^\alpha, \tag{32}$$

where θ^α is the angle between the trace normal $\mathbf{N}^\alpha$ and the surface normal $\mathbf{n}$, while ϕ^α determines edge/screw nature of dislocations piled-

up against the boundary.

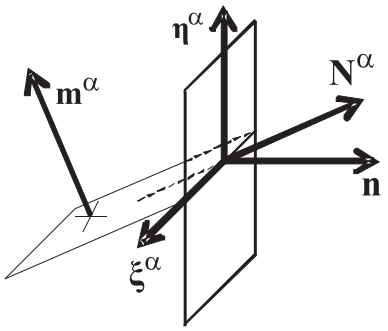

Figure 7: Geometry of an interface and the slip plane intersecting it.

Consider the configuration with stacked pile-ups (Figure 5). Densely packed dislocations at the boundary are represented by the jump in the slip, or equivalently, the Dirac delta function for the slip gradient. In the discrete representation, this represents a wall of super-dislocations at the boundary. Thus, the slip jump at the boundary, $\Delta\gamma^\alpha$, represents the line density of Burgers vector, given per unit length of in the direction η^α (Figure 7) orthogonal to the intersection of boundary and stacked slip planes:

$$\mathbf{B}^\alpha = \Delta\gamma^\alpha \cos\theta^\alpha \zeta_\circ^\alpha. \tag{33}$$

The factor $\cos\theta^\alpha$ arises from the relation between the slip plane spacing h^α (Figure 5) and the spacing of boundary intersections of the same slip planes. To compute the energy, we need the description that distinguishes between screw and edge pile-ups:

$$\mathbf{\Gamma}^\alpha = \mathbf{B}^\alpha \cdot (\zeta_\circ^\alpha \mathbf{N}^\alpha) = \Delta\gamma^\alpha \cos\theta^\alpha \mathbf{N}^\alpha. \tag{34}$$

With such kinematic description, the coarsening error in microstructural energy can be represented in terms of continuum fields $\mathbf{g}^\alpha$ and $\mathbf{\Gamma}^\alpha$. The expression for the *total* coarsening error in microstructural energy *for the single slip case* can be written as:

$$\Delta W^m = \frac{1}{2}\int_V \mathbf{g}^\alpha \cdot \mathbf{D}^{\alpha\alpha} \cdot \mathbf{g}^\alpha dV + \frac{1}{2}\int_S \mathbf{\Gamma}^\alpha \cdot \mathbf{F}^{\alpha\alpha} \cdot \mathbf{\Gamma}^\alpha dS. \tag{35}$$

The constitutive tensors $\mathbf{D}^{\alpha\alpha}$ and $\mathbf{F}^{\alpha\alpha}$ have been derived from dislocation mechanics (Mesarovic et al, 2010). They depend on elastic constants and the slip plane spacing h^α. The components of $\mathbf{F}^{\alpha\alpha}$are proportional to the slip plane spacing, h^α, $\mathbf{D}^{\alpha\alpha}$ are proportional to $(h^\alpha)^2$. All components are given in the Appendix.

7 Size-dependent continuum theory without relaxation

The problem of interaction energies between dislocations on multiple slip systems is significantly simplified by the local nature of the coarsening error in microstructural energy; the orientation dependence of interaction energy between two segments can be separated from its distance dependence. Such orientation dependence can be obtained either from interaction of discrete dislocation segments (Hirth & Lothe, 1992), or from the expression for microstructural energy used here (2, 26):

$$\begin{aligned}\Delta W^m &= \frac{1}{2}\int_V \sum_{\alpha,\beta} \mathbf{g}^\alpha \cdot \mathbf{D}^{\alpha\beta} \cdot \mathbf{g}^\beta dV + \frac{1}{2}\int_S \sum_{\alpha,\beta} \mathbf{\Gamma}^\alpha \cdot \mathbf{F}^{\alpha\beta} \cdot \mathbf{\Gamma}^\beta dS \\ &= \frac{1}{2}\int_V \sum_{\beta} \mathbf{p}^\beta \cdot \mathbf{g}^\beta dV + \frac{1}{2}\int_S \sum_{\beta} \mathbf{q}^\beta \cdot \mathbf{\Gamma}^\beta dS \end{aligned} \tag{36}$$

The energy conjugates are given as

$$\mathbf{p}^\alpha = \sum\nolimits_\beta \mathbf{D}^{\alpha\beta} \cdot \mathbf{g}^\beta,\ \mathbf{q}^\alpha = \sum\nolimits_\beta \mathbf{F}^{\alpha\beta} \cdot \mathbf{\Gamma}^\beta. \tag{37}$$

We note that for the multi-slip case, the energy conjugates $\mathbf{p}^\alpha$ and $\mathbf{q}^\alpha$ do not, in general, lie in the slip plane α. The constitutive tensors $\mathbf{D}^{\alpha\beta}$ and $\mathbf{F}^{\alpha\beta}$ are given in the Appendix.

The weak form (virtual work principle) of the size-dependent crystal plasticity can be written as

$$\begin{aligned}\delta W &= \int_V \left[\sigma : \delta\mathbf{e} + \sum\nolimits_\alpha \tau^\alpha \left|\delta\gamma^\alpha\right| + \sum\nolimits_\alpha \mathbf{p}^\alpha \cdot \delta\mathbf{g}^\alpha\right] dV \\ &\quad + \int_S \sum\nolimits_\alpha \mathbf{q}^\alpha \cdot \delta\mathbf{\Gamma}^\alpha dS = \int_S \mathbf{t} \cdot \delta\mathbf{u} dS. \end{aligned} \tag{38}$$

The summations in the integrand take place over all currently active slip systems. The definition of an active slip system will follow from the analysis of (38). Following Gurtin's (2000, 2002) analysis, the work conjugate of slip, τ^α, is not directly related to the resolved shear stress as in the size-invariant theory. It is considered independent material parameter.

We note that virtual displacements $\delta\mathbf{u}$, and virtual slips, $\delta\gamma^\alpha$, cannot be considered truly independent. More precisely, if one wishes to impose a variation $\delta\gamma^\alpha \neq 0$, $\delta\gamma^{\beta\neq\alpha} = 0$, $\delta u_i = 0$, the variation $\delta\gamma^\alpha$ must be subject to additional constraint of constant average slip in each slip plane. The average value can vary in the direction orthogonal to the slip plane. The details of the analysis of the variational problem (38) are given in Mesarovic et al (2010). The final result is the strong form of the boundary value problem, which includes the standard, simple continuum PDEs and boundary conditions:

$$\begin{array}{l} \nabla \cdot \sigma = 0 \text{ in } V, \\ \mathbf{n} \cdot \sigma = \mathbf{t} \text{ on } S, \end{array} \tag{39}$$

and the additional set of differential equations for each active slip plane:

$$\left\{ \begin{array}{l} \overset{\alpha}{\nabla} \cdot \mathbf{p}^\alpha = \tau^\alpha - \tau_R^\alpha \text{ in } V \\ \\ \mathbf{N}^\alpha \cdot (\mathbf{p}^\alpha + \mathbf{q}^\alpha) = 0 \text{ on } S \end{array} \right\}, \ \alpha = 1, 2, ... \tag{40}$$

We emphasize that the boundary conditions in (40) are, in fact, internal; they are determined by the constitutive equations (A2). No higher order boundary conditions are needed.

Let the number of active slip systems be n_s. Then (39, 40) represent a set of $(3 + n_s)$ second order partial differential equations for $(3 + n_s)$ unknown fields: $u_i(\mathbf{x})$, $i = 1, 2, 3$, and $\gamma^\alpha(\mathbf{x})$, $\alpha = 1, 2, ..., n_s$, endowed with appropriate boundary conditions. For each slip system, equations (38) taken alone, represent a two-dimensional problem in the slip plane, with mixed boundary conditions.

Finally, to recast the formulation in the standard plasticity form with the yield condition, we note that the first equation in (38) is valid for

active slip systems ($\delta\gamma^\alpha \neq 0$). If

$$\left|\overset{\alpha}{\nabla}\cdot\mathbf{p}^\alpha(\mathbf{x}) + \tau_R^\alpha(\mathbf{x})\right| < \tau^\alpha(\mathbf{x}), \tag{41}$$

then the slip system α is inactive at point $\mathbf{x}$, i.e., $\delta\gamma^\alpha(\mathbf{x}) = 0$. The case $\left|\overset{\alpha}{\nabla}\cdot\mathbf{p}^\alpha + \tau_R^\alpha\right| > \tau^\alpha$ is not admissible. The dissipative term $\sum_\alpha \tau^\alpha \left|\delta\gamma^\alpha\right|$ in (38), includes the current flow stress for the slip system α, τ^α. In standard plasticity, the evolution of τ^α with slip is addressed by introducing phenomenological models for statistical hardening, but such issues are beyond scope of this paper.

Finally, consider an impenetrable interface between two plastically deforming solids, with identical isotropic elastic properties. The localized nature of the coarsening error in microstructural energy (36) enables local representation of the interactions between pile-ups on both sides of the boundary through the boundary slips $\mathbf{\Gamma}^\alpha$. All that is required is to state that the sums over index βgn (36), and in constitutive laws (A2), now include *summation over all slip systems involved in pile-ups on both sides of the interface.* The theory is thus generalized to composites and polycrystals, but with grain boundaries impenetrable to dislocations.

8 Boundary relaxation and dissipation

As discussed in Section 2, dislocation segments react in the bulk and along the boundary. Moreover, dislocations piled-up against the boundary may react with intrinsic defects which describe the structure of the boundary, or be absorbed by the boundary and dissociate into various sessile and mobile products. The dislocations in the bulk are represented by densities $\mathbf{g}^\alpha$, while those piled-up in thin boundary layer are represented by $\mathbf{\Gamma}^\alpha/h^\alpha$. Since, in general, $\mathbf{g}^\alpha \ll \mathbf{\Gamma}^\alpha/h^\alpha$, it seems reasonable to assume that the reactions in the bulk occur will much smaller probability then those at the interface, and may, as the first approximation, be neglected. Consequently, we focus on interface reactions.

When two plastically deforming crystals are interfaced, dislocation segments in boundary layers can undergo complex reactions. The typical

result is partial annihilation of Burgers vectors on the two sides of the interface and formation of extra dislocation walls. From the continuum point of view, the conditions that preserve the total Burgers vector have been studied by Gurtin & Needleman (2005).

In general, the criteria for reactions depend on the atomic scale considerations. For twist boundaries, the reactions will strongly depend on the mobility of atoms at the interface. Even at tilt boundaries, the slip planes in general are out of register; recall that different slip systems are characterized by different slip plane spacings h^α. Therefore, there will be kinetic barriers to interface reactions, i.e., threshold conditions in rate-independent formulation. Such barriers/thresholds require atomic scale analysis. In the present work, we ignore this class of problems and concentrate on continuum thermodynamics. However, the resulting theory does not preclude additional interface reaction conditions.

In the present case, the net Burgers vector density is defined directly from (33) for each slip system. The duality between the Burgers vector density and the slip jump vector follows from (33, 34):

$$\boldsymbol{\Gamma}^\alpha = \mathbf{B}^\alpha \cdot (\zeta_\circ^\alpha \mathbf{N}^\alpha), \ \mathbf{B}^\alpha = \boldsymbol{\Gamma}^\alpha \cdot (\mathbf{N}^\alpha \zeta_\circ^\alpha) \tag{42}$$

Both, $\boldsymbol{\Gamma}^\alpha$ and $\mathbf{B}^\alpha$ are dimensionless quantities, since both represent densities of Burgers vector per unit length in the direction η^α (Figure 7).

Consider two slip systems and two corresponding Burgers vector densities, I and II, either on the same or on different sides of the interface. The two Burgers vector densities are defined with respect to line directions (cf. Figure 2): $(\xi^I, \mathbf{B}^I)$ and $(\xi^{II}, \mathbf{B}^{II})$. Since the numbers of actual dislocation lines belonging to two slip systems are, in general, different, only a portion of $\mathbf{B}^I$ will relax by reacting with other system. Denote the relaxed portion as $\widehat{\mathbf{B}}^I$; the unrelaxed portion is then

$$\bar{\mathbf{B}}^I = \mathbf{B}^I - \widehat{\mathbf{B}}^I, \ \bar{\boldsymbol{\Gamma}}^\alpha = \boldsymbol{\Gamma}^\alpha - \widehat{\boldsymbol{\Gamma}}^\alpha. \tag{43}$$

8.1 Slip systems with parallel traces

Consider first the case when slip plane traces of the two systems are parallel. This is the simplest case, and the geometry of the product

is easily established. In fact, the analysis presented below is, at the continuum level equivalent to several different discrete events, illustrated in Figure 8 (disconnection in Figure 8(a) notwithstanding).

The line direction of the product ξ^R will be parallel to the line directions of reacting dislocations. One can arbitrarily choose $\xi^R = \xi^I$. The products Burgers vector is then:

$$\mathbf{B}^R = \widehat{\mathbf{B}}^I + (\xi^{II} \cdot \xi^I)\widehat{\mathbf{B}}^{II}. \tag{44}$$

It is convenient to regard the product as belonging to a fictitious slip system R:

$$\zeta_\circ^R = \mathbf{B}^R / \left|\mathbf{B}^R\right|, \qquad \mathbf{m}^R = \left\{ \begin{array}{ll} \dfrac{\xi^R \times \zeta_\circ^R}{|\xi^R \times \zeta_\circ^R|} & \text{if} \quad \xi^R \times \zeta_\circ^R \neq 0 \\ \mathbf{n} & \text{otherwise} \end{array} \right\},$$

$$\mathbf{P}^R = \mathbf{I} - \mathbf{m}^R\mathbf{m}^R, \qquad \mathbf{N}^R = \frac{\mathbf{P}^R \cdot \mathbf{n}}{|\mathbf{P}^R \cdot \mathbf{n}|}, \qquad \mathbf{\Gamma}^R = \mathbf{B}^R \cdot (\zeta_\circ^R \mathbf{N}^R). \tag{45}$$

The free energy of the relaxed system is now determined by the unrelaxed portions $\bar{\mathbf{\Gamma}}^\alpha$, and the product $\mathbf{\Gamma}^R$:

$$\begin{aligned} \Phi \;\; = \;\; & \frac{1}{2}\int_V \left\{ \mathbf{e} : \mathbf{C} : \mathbf{e} + \sum_{\alpha,\beta} \mathbf{g}^\alpha \cdot \mathbf{D}^{\alpha\beta} \cdot \mathbf{g}^\beta \right\} dV \\ & + \frac{1}{2}\int_S \sum_{\alpha',\beta'} \bar{\mathbf{\Gamma}}^{\alpha'} \cdot \mathbf{F}^{\alpha'\beta'} \cdot \bar{\mathbf{\Gamma}}^{\beta'} dS. \end{aligned} \tag{46}$$

Symbolically, the primed indices indicate that the summation is taken over all slip systems on both sides of the interface (unrelaxed portions), and over all fictitious systems (44, 45). The definition of constitutive tensors $\mathbf{F}^{\alpha'\beta'}$ (A2) and work-conjugates $\mathbf{q}^{\alpha'}$ (37) is extended accordingly to include the fictitious systems. For that purpose a characteristic spacing h^R is needed. It can be determined as a weighted average of the spacings in slip systems involved in reaction:

$$\left|\widehat{\mathbf{B}}^I\right| h^I + \left|\widehat{\mathbf{B}}^{II}\right| h^{II} = \left|\mathbf{B}^R\right| h^R \quad . \tag{47}$$

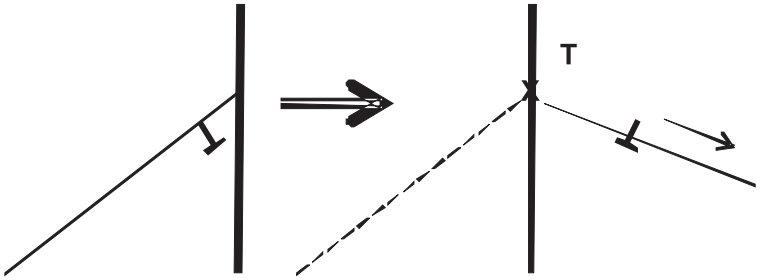

(a) Dislocation impinges on a boundary and nucleates dislocation in the neighboring crystal, leaving a sessile dislocation and a disconnection. The latter produces steps on the interface, but we ignore it at this level of analysis.

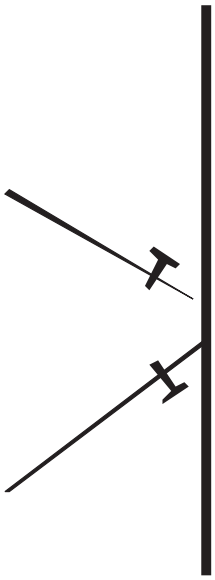

(b) Two dislocations from the same crystal meet at the interface.

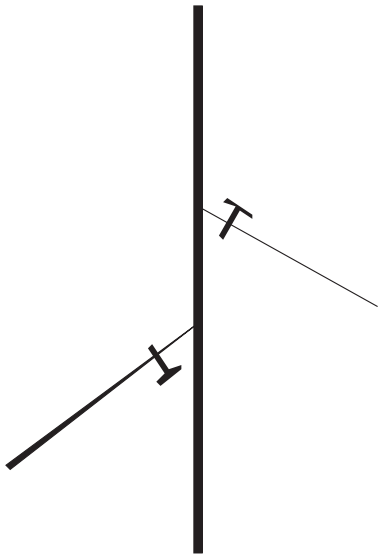

(c) Dislocations on two sides of the interface impinge on the interface and react.

Figure 8: The discrete events covered by the analysis presented in Section 8.1.

On the level of dislocation mechanics, the boundary relaxation can occur either as a reaction between piled-up dislocations on two slip systems, or, by nucleation of a dislocation loop at the boundary, on say, side *II*, as a result of the pile-up at side I, and subsequent (fast) propagation of nucleated loop through the solid *II*. From the point of view of continuum kinematics, which is oblivious to the position of the source, these two cases are equivalent. The relaxation occurs by a series of atomic level steps which can only be quantified by atomic level calculations. Pending such results, we assume that boundary relaxation occurs as soon as it is kinematically possible and thermodynamically consistent.

Dissipative events in dislocation motion typically involve a passage through a high energy configuration, followed by relaxation. The difference in energies between the peak energy configuration and the final relaxed state is considered dissipated[18]. The relaxed portions of slip steps $\widehat{\mathbf{\Gamma}}^{I}$ and $\widehat{\mathbf{\Gamma}}^{II}$ now enter the rate of dissipation, which is given as

$$D = \int_V \sum\nolimits_\alpha \tau^\alpha \, |\dot{\gamma}^\alpha| dV + \int_S dS \sum\nolimits_R \sum\nolimits_{I,II} \left[\mathbf{k}^{R,I} \cdot \dot{\widehat{\mathbf{\Gamma}}}^{I} + \mathbf{k}^{R,II} \cdot \dot{\widehat{\mathbf{\Gamma}}}^{II} \right] \tag{48}$$

The dissipation work conjugates $\mathbf{k}^{R,I}$ and $\mathbf{k}^{R,II}$, derived in (Mesarovic et al, 2010), are given in the Appendix.

The reaction between systems I and II will occur only if it lowers the free energy of the system, i.e. if the dissipation rate is positive. Consider small increments in relaxed boundary slips be denoted $\delta\widehat{\mathbf{\Gamma}}^{I}$ and $\delta\widehat{\mathbf{\Gamma}}^{II}$. The free energy in the final (relaxed) state is the quadratic form of $(\bar{\mathbf{\Gamma}}^{I}, \bar{\mathbf{\Gamma}}^{II}, \delta\mathbf{\Gamma}^{R})$. The condition that dissipation must be positive reads:

$$\mathbf{q}^{I} \cdot \delta\widehat{\mathbf{\Gamma}}^{I} + \mathbf{q}^{II} \cdot \delta\widehat{\mathbf{\Gamma}}^{II} - \mathbf{q}^{R} \cdot \delta\mathbf{\Gamma}^{R} \geq 0. \tag{49}$$

This is the realization of the 2^{nd} law of thermodynamics (Clausius-Duhem inequality) for isothermal processes.

[18] Consider, e.g., the problem of a dislocation passing another parallel pinned dislocation.

The only remaining question is how to determine the portion of the slip step increment that is relaxed. For that purpose, denote:

$$\delta\widehat{\mathbf{\Gamma}}^{I} = \alpha^{I}\delta\mathbf{\Gamma}^{I},\ \delta\widehat{\mathbf{\Gamma}}^{II} = \alpha^{II}\delta\mathbf{\Gamma}^{II}. \tag{50}$$

Assuming that the system minimizes free energy, i.e., maximizes dissipation, α^{I} and α^{II} can be found as the combination that maximizes the left-hand-side of (49).

8.2 Slip systems of with non-parallel traces

The illustration of the problem is shown in Figure 1(c). Two non-parallel sets of dislocations impinge on the interfaces. The increased mobility at the interface allows the structure to relax, i.e., to lowers its energy. The resulting structure could be periodic or quasiperiodic, as long as the range of material transport is limited.

The 2D periodic structure is characterized by two translation vectors (cf. Figures 5 and 7) $(\eta^{I}h^{I}/\cos\theta^{I},\ h^{II}\eta^{II}/\cos\theta^{II})$, where

$$\eta^{\alpha} = \xi^{\alpha} \times \mathbf{n}. \tag{51}$$

Any periodic structure that decreases the free energy of the system is possible. The initial and the relaxed structure must satisfy the surface conservation of total Burgers vector in the periodic cell. Let S_0 be the area of the parallelogram encompassed by the two translation vectors (Figure 9). Then:

$$\int_{S_0} \left[\mathbf{B}^{I}\xi^{I} + \mathbf{B}^{II}\xi^{II}\right] dS_0 = const. \tag{52}$$

The free energy of the system is determined by the relaxed configuration. The dissipation is the difference in free energy between the original configuration and the relaxed one.

At present, we have no way of predicting the relaxed configuration, except by atomistic studies. However, once the relaxed configuration is determined, the free energy is easily estimated using the methods of linear elasticity.

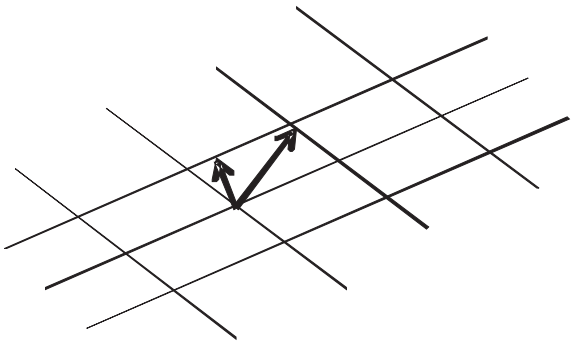

Figure 9: Two sets of dislocations impinging on a boundary, and the two translation vectors for the relaxed periodic lattice. The translation vectors are orthogonal to dislocation lines and have a magnitude equal to the spacings of slip planes in the two systems.

8.3 Dislocations absorbed by the boundary

The general case is shown in Figure 1(a) (down). Dislocation absorbed by the boundary may (Priester, 2001):

(i) Relax by extending its core, or,

(ii) Dissociate into partials, one of which may be mobile.

As before, the prediction of the mechanism can only be affected by atomistic simulations. Once that is accomplished, energies are computed using linear elasticity.

Finally, it bears emphasis that the list of outcomes discussed in Sections 8.1-3 may not be complete. It is simply a list of reactions observed at the boundaries so far. The main point of the above discussion is that once criteria for determining the type of dislocation-interface reactions are available, the continuum framework outlined above can accommodate them.

9 Summary and discussion

We have summarized the recent advances in continuum plasticity of crystals, and, discussed the unsolved problems in plasticity of interfaces.

First, we considered systems without boundary dissipation (relaxation). Once the energy landscape is defined, the dissipation model for the boundaries is defined from the height of energy barriers (peak energy configurations).

The resulting rate-independent (quasistatic) continuum crystal plasticity theory is size-dependent. The characteristic lengths are the average slip plane spacing for each slip system. They may evolve through the double-cross slip mechanism. The theory features the slip-dependent interface free energy and interface dissipation for penetrable interfaces.

The analysis in this paper is based on linearized kinematics and isotropic elasticity with no elastic mismatch between adjacent crystals. The generalization to arbitrary kinematics should present no conceptual problems. Consideration of elastic anisotropy first requires a mathematical development similar to the one in Mesarovic (2005), i.e., the integral formulation of dislocation interaction energies. The exact treatment of elastic mismatch is difficult, but an approximation is simple.

Plastic relaxation at grain boundaries and interfaces represent a more difficult and yet unsolved problem. In this paper, we have only outlined a framework in which the problems of dislocation-boundary interactions can be considered. The criteria for deciding which interface reaction takes place are not available at present. To produce such criteria, a systematic investigation and mapping of the interface orientation space is needed using atomistic simulations.

Appendix

The constitutive tensors for the single slip t no relaxation theory (35) are given by:

$$\begin{aligned} \mathbf{D}^{\alpha\alpha} &= h^{\alpha 2}[d_{\perp}\zeta_{\circ}^{\alpha}\zeta_{\circ}^{\alpha} + d_{\circ}\zeta_{\perp}^{\alpha}\zeta_{\perp}^{\alpha}], \\ \mathbf{F}^{\alpha\alpha} &= h^{\alpha}[f_{\perp}^{2}d_{\perp}\zeta_{\circ}^{\alpha}\zeta_{\circ}^{\alpha} + f_{\circ}^{2}d_{\circ}\zeta_{\perp}^{\alpha}\zeta_{\perp}^{\alpha}]. \end{aligned} \tag{A1}$$

with: $d_{\perp} = \bar{E}/12$, and $d_{\circ} = \mu/12$. The coefficients $f_{\perp} \approx 9/4$ and $f_{\circ} \approx 3$ are computed by comparing the numerical solutions of the semi-discrete problem to the solution of the continuum theory.

For multiple slip - no relaxation theory (36, 37, 46), the constitutive tensors are ():

$$\begin{aligned} \mathbf{D}^{\alpha\beta} &= \frac{1}{2}h^{\alpha}h^{\beta}\left[\mathbf{D}_{\perp\perp}^{\alpha\beta} + \mathbf{D}_{\perp\circ}^{\alpha\beta} + \mathbf{D}_{\circ\perp}^{\alpha\beta} + \mathbf{D}_{\circ\circ}^{\alpha\beta}\right], \\ \mathbf{F}^{\alpha\beta} &= \frac{1}{2}\sqrt{h^{\alpha}h^{\beta}}\left[f_{\perp}^{2}\mathbf{D}_{\perp\perp}^{\alpha\beta} + f_{\perp}f_{\circ}\mathbf{D}_{\perp\circ}^{\alpha\beta} + f_{\circ}f_{\perp}\mathbf{D}_{\circ\perp}^{\alpha\beta} + f_{\circ}^{2}\mathbf{D}_{\circ\circ}^{\alpha\beta}\right], \end{aligned} \tag{A2}$$

for $\alpha \neq \beta$, with:

$$\begin{bmatrix} \mathbf{D}_{\perp\perp}^{\alpha\beta} & \mathbf{D}_{\perp\circ}^{\alpha\beta} \\ \mathbf{D}_{\circ\perp}^{\alpha\beta} & \mathbf{D}_{\circ\circ}^{\alpha\beta} \end{bmatrix} = \begin{bmatrix} d_{\perp}(\mathbf{m}^{\alpha}\cdot\mathbf{m}^{\beta})\zeta_{\circ}^{\alpha}\zeta_{\circ}^{\beta} & d_{\perp}(\zeta_{\circ}^{\alpha}\cdot\zeta_{\circ}^{\beta})(\zeta_{\perp}^{\alpha}\cdot\zeta_{\circ}^{\beta})\zeta_{\circ}^{\alpha}\zeta_{\perp}^{\beta} \\ d_{\perp}(\zeta_{\circ}^{\beta}\cdot\zeta_{\circ}^{\alpha})(\zeta_{\perp}^{\beta}\cdot\zeta_{\circ}^{\alpha})\zeta_{\perp}^{\alpha}\zeta_{\circ}^{\beta} & d_{\circ}\left[(\zeta_{\circ}^{\alpha}\cdot\zeta_{\circ}^{\beta})^{2}-1\right]\zeta_{\perp}^{\alpha}\zeta_{\perp}^{\beta} \end{bmatrix} \tag{A3}$$

Dissipative work-conjugates, for the case of parallel slip traces (48) are:

$$\begin{aligned} \mathbf{k}^{I,R} &= \mathbf{q}^{I} - \mathbf{q}^{R}\cdot(\mathbf{N}^{R}\zeta_{\circ}^{R})\cdot(\zeta_{\circ}^{I}\mathbf{N}^{I}), \\ \mathbf{k}^{II,R} &= \mathbf{q}^{II} + \mathbf{q}^{R}\cdot(\mathbf{N}^{R}\zeta_{\circ}^{R})\cdot(\zeta_{\circ}^{II}\mathbf{N}^{II}). \end{aligned} \tag{A4}$$

References

[1] Adams, B.L. & Field, D.P. 1992 Measurement and representation of grain boundary texture. *Metall. Trans.*, **23A**, 2501-2513.

[2] Adams, B.L., Kinderlehrer, D., Livshits, I., Mason, D.E., Mullins, W.W., Rohrer, G.S., Rollett, A.D., Saylor, D.M., Ta'asan, S. & Wu, C-t. 1999 Extracting grain boundary and surface energy from measurement of triple junction geometry. *Interface Science* **7,** 321-337.

[3] Aifantis, E.C. 1987 The physics of plastic deformation. *Int. J. Plasticity* **3**, 211-247.

[4] Aifantis, K.E. & Willis, J.R., 2005. The role of interfaces in enhancing the yield strength of composites and polycrystals. *J. Mech. Phys. Solids* **53**, 1047–1070.

[5] Akarapu, S., Zbib, H.& Hirth, J.P. 2008 Modeling and analysis of disconnections in tilt walls. *Scripta Mater.* 59(3), 265-67.

[6] Arsenlis, A., Parks, D.M., Becker, R. & Bulatov, V.V. 2004 On the evolution of crystallographic dislocation density in non-homogeneously deforming crystals. *J. Mech. Phys. Solids* **52**, 1213-1246.

[7] Asaro, R.J. & Rice J.R. 1977 Strain localization in ductile single crystals. *J. Mech. Phys. Solids* **25**, 309.

[8] Ashby, M.F. 1970 The deformation of plastically non-homogeneous materials. *Phil. Mag.* **21**, 399-424.

[9] Baskaran, R., Akarapu, S., Mesarovic, S. & Zbib, H.M. 2010 Energies and distributions of dislocations in stacked pile-ups. *Int. J. Solids Structures* **47,** 1144-1153.

[10] Bassani, J.L. 1994 Plastic Flow of Crystals. Adv. App. Mech. 30, 191-257.

[11] Bassani, J.L., Needleman, A. & Van der Giessen, E. 2001 Plastic flow in a composite: a comparison of nonlocal continuum and discrete dislocation predictions. *Int. J. Solids Structures* **38**, 833-853.

[12] Bassani, J. L. & Wu T. Y. 1989. Latent hardening in single crystals. II. Analytical characterization and predictions. *Proc. Roy. Soc. Lond. A* **435**, 21-41.

[13] Bittencourt, E., Needleman, A., Gurtin, M.E. & Van der Giessen, E. 2003 A comparison of nonlocal continuum and discrete dislocation plasticity predictions. *J. Mech. Phys. Solids* **51**, 281-310.

[14] Bollman, W. 1970 *Crystal defects and crystalline interfaces.* Springer, Berlin.

[15] Bridgman, P.W. 1923 The compressibility of thirty metals as a function of pressure and temperature. *Proc. Am. Acad. Arts. Sci.* **58**, 165

[16] Bridgman, P.W. 1949 *The physics of high pressure.* Bell and Sons, London.

[17] Chen, D., Lu, M., Lin, D. & Chen,T.L. 1993 Energy and structural simulations of the interaction between the grain boundary and dislocations in Ni_3Al alloys. *Mater. Sci. Eng. A* **167**, 165-170.

[18] Clark, W.A.T., Wagoner, R.H., Shen, Z.Y., Lee, T.C., Robertson, I.M. & Birnbaum, H.K. 1992 On the criteria for slip transmission across interfaces in polycrystals. *Scripta Metall. Mater.* **26**(2), 203-6.

[19] Couzinié, J.P., Decamps, B. & Priester, L. 2003 On the interactions between dislocations and a near-Σ=3 grain boundary in a low stacking-fault energy metal. *Phil. Mag. Letters* 83(12), 721-731.

[20] Couzinié, J.P., Décamps, B. & Priester, L. 2005 Interaction of dissociated lattice dislocations with a Σ=3 grain boundary in copper. *Int. J. Plasticity* 21(4), 759-775.

[21] Couzinié, J.P., Decamps, B. & Priester, L. 2004 On the first steps of grain boundary dislocation stress relaxations in copper. *Zeitschrift fuer Metallkunde* 95(4), 223-225.

[22] Cuitino, A.M. & Ortiz, M. 1993 Computational modeling of single crystals. *Mod. Simul. Mater. Sci. Eng.* **1**(3), 225–263.

[23] De Guzman, M.S., Neubauer, G., Flinn, P. & Nix, W.D. 1993 The role of indentation depth on the measured hardness of materials. *Mater. Res. Symp. Proc.* **308**, 613-618.

[24] Dillon, S. J., Harmer, M. P. & Rohrer, G.S. 2010 The Relative Energies of Normal and Abnormal Grain Boundaries Displaying Different Complexions, *J. Am. Ceram. Soc.* **93**, 1796-1802.

[25] Ewing, J.A. & Rosenhain, W. 1900 The crystalline structure of metals. *Philos. Trans. R. Soc. Lond.* **193**, 353-375.

[26] Field, D.P. & Adams, B.L. 1992 Interface Cavitation Damage in Polycrystalline Copper. *Acta Metall. et Mater*, **40**, 1145-1157.

[27] Fleck, N.A. & Hutchinson, J.W. 1993 A phenomenological theory for strain gradient effects in plasticity. *J. Mech. Phys. Solids* **41**, 1825-57.

[28] Fleck, N.A. & Hutchinson, J.W. 1997 Strain gradient plasticity. *Adv. Appl. Mech.* **33**, 295-362.

[29] Fleck, N.A., Muller, G.M., Ashby, M.F. & Hutchinson, J.W. 1994 Strain gradient plasticity: Theory and experiment. *Acta metal. mater.* **42**(2), 475-87.

[30] Fleck, N.A. & Willis, J.R. 2009 A mathematical basis for strain-gradient plasticity theory—Part I: Scalar plastic multiplier. *J. Mech. Phys. Solids* **57**, 161-77.

[31] Fortes, M.A. 1972 Grain boundary parameters. *Acta Cryst. A* **28**, 100-102.

[32] Frank, F.C. & Read, W.T. 1950 Multiplication processes for slow moving dislocations. *Phys. Rev.* **79**, 722-724.

[33] Franciosi, P., Berveiller, M. & Zaoui, A. 1980 Latent hardening in copper and aluminium single crystals, *Acta Metall.* **28**, p. 273.

[34] Franciosi, P. & Zaoui, A. 1982 Multislip in F. C. C. crystals: A theoretical approach compared with experimental data, *Acta Metall.* **30**, p. 1627.

[35] Franciosi, P. 1983 Glide mechanisms in B. C. C. crystals: and investigation of the case of a-iron through multislip and latent hardening tests, *Acta Metall.* **31**, 1331.

[36] Franciosi, P. 1985 The concepts of latent hardening and strain hardening in metallic single crystals. *Acta Metall.* **33**, 1601.

[37] Fredriksson, P. & Gudmundson, P. 2007 Competition between interface and bulk dominated plastic deformation in strain gradient plasticity. *Mod. Simul. Mater. Sci. Eng.* **15**(1), S61–S69.

[38] Frenkel, L. 1926 Zur Theorie der Plastizitätgremze und der gestigheit kristallinischer Körper. *Z. Physik A* **37**, 572-609.

[39] Gane, N., Cox, J.M. 1970 The micro-hardness of metals at very low loads. *Phil. Mag.* **22**, 881-891.

[40] Groma, I. 1997 Link between the microscopic and mesoscopic length-scale description of the collective behaviour of dislocations. *Phys. Rev. B* **56**, 5807-5813.

[41] Groma, I., Csikor, F. & Zaiser, M. 2003 Spatial correlations and higher-order gradient terms in a continuum description of dislocation dynamics. *Acta Mater.* **51**, 1271-1281.

[42] Groma I., Gyorgyi G. & Kocsis B. 2006 Debye screening of dislocations, *Phys. Rev. Lett.* **96**, 165503

[43] Groma I., Gyorgyi G. & Kocsis B. 2007 Dynamics of coarse grained dislocation densities from an effective free energy, *Phil. Mag.* **87**, 1185-1199.

[44] Gudmundson, P. 2004 A unified treatment of strain gradient plasticity. *J. Mech. Phys. Solids* **52**, 1379–1406.

[45] Gurtin, M.E. 2000 On the plasticity of single crystals: free energy, microforces, plastic strain gradients. *J. Mech. Phys. Solids* **48**, 989-1036.

[46] Gurtin, M.E. 2002 A gradient theory of single-crystal viscoplasticity that accounts for geometrically necessary dislocations. *J. Mech. Phys. Solids* **50**, 5-32.

[47] Gurtin, M.E. 2003 On a framework for small-deformation viscoplasticity: free energy, microforces, strain gradients. *Int. J. Plasticity* **19**, 47-90.

[48] Gurtin, M.E. & Needleman, A. 2005 Boundary conditions in small-deformation, single crystal plasticity that account for the Burgers vector. *J. Mech. Phys. Solids* **53**, 1-31.

[49] Hall, E. O. 1951 The Deformation and Ageing of Mild Steel: III Discussion of Results**.** *Proc. Phys. Soc. B* **64** 747-753.

[50] Hill, R. 1966 Generalized constitutive relations for incremental deformation of metals by multislip. *J. Mech. Phys. Solids* **14**, 99.

[51] Hill, R. & Havner, K.S. 1982 Perspectives in the mechanics of elastoplastic crystals. *J. Mech. Phys. Solids* **30**, 5.

[52] Hill, R. & Rice J.R. 1972 Constitutive analysis of elasto-plastic crystals at arbitrary strain. *J. Mech. Phys. Solids* **20**, 401.

[53] Hirth, J.P. & Lothe, J. 1992 *Theory of Dislocations*. Reprint of the 2^{nd} edition (1982). Wiley, New York.

[54] Hirth, J.P., Pond, R.C. & Lothe, J. 2006_Disconnections in tilt walls. *Acta Mater.* **54**(16), 4237-4245.

[55] Hirth, J.P., Pond, R.C. & Lothe, J. 2007 Spacing defects and disconnections in grain boundaries. *Acta Mater* **55**, 5428–5437.

[56] Hirth, J.P., Rhee, M. & Zbib, H.M. 1996 Modeling of deformation by a 3D simulation of multiple, curved dislocations. *J. Computer-Aided Materials Design* **3,** 164-166.

[57] Khraishi, T.A. & Zbib, H.M. 2002a Dislocation dynamics simulations of the interaction between a short rigid fiber and a glide circular dislocation pile-up. *Comp. Mater. Science* **24**, 310-322.

[58] Khraishi, T.A. & Zbib, H.M. 2002b Free surface effects in 3D dislocation dynamics: Formulation and modeling. *J. Eng. Mater. Techn.* **124**, 342-351.

[59] Kosevich, A.M. 1979 Crystal dislocations and the theory of elasticity. In *Dislocations in Solids, Vol.* **1**, 33-141. Ed. F.R.N. Nabarro. North–Holland Publishing Co.

[60] Kröner, E. 1958 Kontinuumstheorie der Versetzungen und Eigenspannungen. Ergeb. *agnew. Math.* **5**. Springer-Verlag

[61] Kröner, E. 1981 Continuum theory of defects. In *Les Houches, Session XXXV - Physics of defects*, R. Balian et al. (eds.) , North-Holland, Amsterdam, pp. 217–315.

[62] Limkumnerd S, Van der Giessen E. 2008 Study of size effects in thin films by means of a crystal plasticity theory based on DFT, *J Mech Phys Solids* **56**, 3304-3314.

[63] Ma, Q. & Clarke, D.R. 1995 Size dependent hardness of silver single crystals. *J. Mater. Res.* **10**(4), 853-863.

[64] McDowell, D.L. 2008 Viscoplasticity of heterogeneous metallic materials. *Mat. Sci. Eng. R* **62**(3), 67-123.

[65] McDowell, D.L. 2010 A perspective on trends in Multiscale plasticity. *Int. J. Plasticity* **26**, 1280-1309.

[66] Mesarovic, S. Dj. 2005 Energy, configurational forces and characteristic lengths associated with the continuum description of geometrically necessary dislocations. *Int. J. Plasticity* **21**, 1855-1889.

[67] Mesarovic, S.Dj., Baskaran, R. & Panchenko, A. 2010 Thermodynamic coarse-graining of dislocation mechanics and the size-dependent continuum crystal plasticity. *J. Mech. Phys. Solids* **58** (3), 311-329.

[68] Mindlin, R.D. 1964 Micro-structure in linear elasticity. *Arch. Rat. Mech. Anal.* **16**, 51-78.

[69] Nix, W.D. & Gao, H. 1998 Indentation size effects in crystalline materials: a law for strain gradient plasticity. *J. Mech. Phys. Solids* **46**(3), 411-425.

[70] Nye, J.F. 1953 Some geometrical relations in dislocated crystals. *Acta Metal.* **1**, 153-62.

[71] Ohashi, T. 2004 Three dimensional structures of the geometrically necessary dislocations in matrix-inclusion systems under uniaxial tensile loading. *Int. J. Plasticity* **20**, 1093-1109.

[72] Orowan E. 1934 Zur Kristallplastizität III: Über die Mechanismus des Gleitvorganges *Zeits. f. Physik* **89**, 634-659.

[73] Ortiz, M. & Popov, E.P. 1982 A statistical theory of polycrystalline plasticity. *Proc. Roy. Soc. Lond. A* **379**, 439-458.

[74] Peach, M. & Koehler, J.S. 1950 The forces exerted on dislocation and the stress field produced by them. *Phys. Rev.* **80**, 436-439.

[75] Pestman, B.J., De Hosson, J.T.H, Vitek, V. & Schapink, F.W. 1991 Interaction between lattice dislocations and grain-boundaries in fcc and ordered compounds - a computer-simulation. *Phil. Mag. A* **64**, 951-969.

[76] *Petch*, N J.1953The cleavage strength of polycrystals. *J. Iron Steel Inst.* **174**, 25-28.

[77] Pethica, J.B., Hutchings, R. & Oliver, W.C. 1983 Hardness measurement at penetration depths as small as 20 nm. *Phil. Mag. A* **48**, 593-606.

[78] Pond, R.C., Celotto, S. & Hirth, J.P. 2003 A comparison of the phenomenological theory of martensitic tramsformations with a model based on interfacial defects. *Acta Mater.* **51**, 5385-5398.

[79] Pond, R. C., Ma, X., Hirth, J. P. & Mitchell, T. E. 2007 Disconnections in simple and complex structures. *Phil. Mag.* **87**(33), 5289-5307.

[80] Pond, R.C. & Vlachavas, D.S. 1983 Bicrystallography. *Proc. R. Soc. of Lond. A* **386**(1790), 95-143.

[81] Poole, W.J., Ashby, M.F. & Fleck, N.A. 1996 Micro-hardness of annealed and work-hardened copper polycrystals. *Scripta Mater.* **34**(4), 559-564.

[82] Polanyi, M. 1934 Über eine Art Gitterstörung die einen Kristall plastisch machen könnte, *Z. Physik A* **89**, 660–664.

[83] Poulat, S., Decamps, B. & Priester, L. 1998 Weak-beam transmission electron microscopy study of dislocation accommodation processes in nickel $\Sigma = 3$ grain boundaries. *Phil. Mag. A* 77(6), 1381-1397.

[84] Poulat S., Decamps B., Priester L. & Thibault, J. 2001 Incorporation processes of extrinsic dislocations in singular, vicinal and general grain boundaries in nickel. *Mater. Sci. Eng. A* **309-310**, 483-485.

[85] Priester, L. 2001 "Dislocation-interface" interaction - stress accommodation processes at interfaces. *Mater. Sci. Eng. A* **309-310**, 430-439.

[86] Rickman, J.M. & LeSar, R. 2001 Finite-temperature dislocation interactions. *Phys Rev B* **64**(9), 094106.

[87] Rohrer, G.S. & Miller, H.M. 2010 Topological Characteristics of Plane Sections of Polycrystals. *Acta Mater.* **58**, 3805-3814.

[88] Roy, A., Peerlings, R.H.J., Geers, M.G.D. & Kasyanuk, Y. 2007 Continuum modeling of dislocation interactions: Why discreteness matters? *Mater. Sci. Eng. A* **486**, 653-661.

[89] Shu, J.Y., Fleck, N.A., Van der Giessen, E. & Needleman, A. 2001 Boundary layers in constrained plastic flow: comparison of nonlocal and discrete dislocation plasticity. *J. Mech. Phys. Solids* **49**, 1361-1395.

[90] Smyshlyaev, V.P. & Fleck, N.A. 1996 The role of strain gradients in the grain size effects form polycrystals. *J. Mech. Phys. Solids* **44**, 465-95.

[91] Spearot, D., Jacob, K.I. & McDowell, D.L. 2005 Nucleation of dislocations from [0 0 1] bicrystal interfaces in aluminum. *Acta Mater.* **53**(13), 3579–3589.

[92] Spearot, D.E., Jacob, K.I. & McDowell, D.L. 2007a Dislocation nucleation from bicrystal interfaces with dissociated structure. *Int. J. Plasticity* **23**, 143–160.

[93] Spearot, D.E., Tschopp, M.A., Jacob, K.I. & McDowell, D.L., 2007b Tensile strength of {100} and {110} tilt bicrystal copper interfaces. *Acta Mater.* **55**(2), 75-714

[94] Stelmashenko, N.A., Walls, M.G., Brown, L.M. & Milman Y.V. 1993 Microindentations on W and Mo oriented single crystals: an stm study. *Acta Metall.* **41**(10), 2855-2865.

[95] Stolken, J.S. & Evans, A.G. 1998 A microbend test method for measuring the plasticity length scale. *Acta Mater.* **46**, 5109-5115.

[96] Sun, S., Adams, B.L. & King, W. 2000 Observations of lattice curvature near the interface of a deformed aluminum bicrystal. *Phil. Mag. A* **80**(1), 9-25.

[97] Sutton, A.P & Balluffi, R.W. 1995 Interfaces in crystalline materials. Clarendon Press, Oxford.

[98] Sutton AP & Vitek V. 1983 On the structure of tilt grain-boundaries in cubic metals . III. Generalizations of the struyctural study and implications for the properties of grain boundaries. *Philos. Trans. Roy. Soc. A* **309**, 55-68.

[99] Taylor, G.I. 1934 The mechanism of plastic deformation of crystals, Part I.-Theoretical. Proc. Roy. Soc. Lond. A **145**, 362-404.

[100] Tschopp, M.A., Spearot, D.E. & McDowell, D.L. 2008 Influence of grain boundary structure on dislocation nucleation in fcc metals. In: Dislocations in Solids A. Tribute to F.R.N. Nabarro (Ed.), J.P. Hirth, vol. 14, 43–139.

[101] Yassar, R.S., Mesarovic, S.Dj. & Field, D.P. 2007 Micromechanics of hardening of elastic-plastic crystals with elastic inclusions: I- Dilute concentration. *Int. J. Plasticity* **23**, 1901-1917.

[102] Yefimov, S., Groma, I. & Van der Giessen, E. 2004 A comparison of statistical-mechanics based plasticity model with discrete dislocation plasticity calculations. *J. Mech. Phys. Solids* **52**, 279-300.

[103] Zaiser, M., Carmen Miguel, M. & Groma, I. 2001 Statistical dynamics of dislocation systems: the influence of dislocation-dislocation correlations. *Phys. Rev. B* **64**, 2224102-2224111.

[104] Zbib, H.M., Rhee, M. & Hirth, J.P. 1996 3D Simulation of Curved Dislocations: Discretization and Long Range Interactions. In *Advances in Engineering Plasticity and its Applications*, eds. T. Abe & T. Tsuta, 15-20. Pergamon, NY.

Submitted on September 2010

Plastičnost kristala i medjupovrši: od diskretnih dislokacija ka teoriji kontinuuma zavisnoj od veličine

Prikazani su nedavni istraživa cki rezultati u kontinualnoj plastičnosti kristala (kvazistatička formulacija nezavisna od brzine) na osnovu mehanike dislokacija. Poseban naglasak je stavljen na relaksaciju klizanja na medjupovrši. Ovaj nerešeni problem je na sadašnjem frontu istraživanja u plastičnosti kristalnih materijala. Postavljamo ovde okvir za sledeća istraživanja zasnovana na teoriji razvijenoj za trodimenzioni kristal.

Ova teorija je zasnovana na konceptu geometrijski potrebnih dislokacija, posebno, na konfiguracijama gde dislokacije se nagomilavaju nasuprot medjupovrši. Prosečno rastojanje izmedju ravni klizanja obezbedjuje karakterističnu dužinu teorije. Fizička interpretacija slobodne energije uključuje grešku u energijama elastične relaksacije koje rezultijaju iz grube reprezentacije polja dislokacione gustine.

Kinematika kontinuuma je odredjena činjenicom da dislokaciona nagomilavanja imaju singularni raspored koji nam dozvoljava da prikažemo gusto dislokaciono polje na granici kao jednu superdislokaciju, tojest, skok u polju klizanja. Pridružena ovom skoku je energija medjupovrši koja zavisi od klizanja, što opet čini ovu formulaciju podesnom za analizu mehanizama relaksacije na medjupovrši.

doi:10.2298/TAM1004289M Math.Subj.Class.: 74C15, 74E05, 74E15